

The strange-quark chemical potential as an experimentally accessible "order parameter" of the deconfinement phase transition for finite baryon-density

Apostolos D. Panagiotou and Panayiotis G. Katsas[†]

[†] University of Athens, Physics Department Nuclear and Particle Physics Division, GR-15771 Athens, Hellas

E-mail: apanagio@phys.uoa.gr, pkatsas@phys.uoa.gr

Abstract. We consider the change of the strange-quark chemical potential in the phase diagram of nuclear matter, employing the Wilson loop and scalar quark condensate order parameters, mass-scaled partition functions and enforcing flavor conservation. Assuming the region beyond the hadronic phase to be described by massive, correlated and interacting quarks, in the spirit of lattice and effective QCD calculations, we find the strange-quark chemical potential to change sign: from positive in the hadronic phase - to zero upon deconfinement - to negative in the partonic domain. We propose this change in the sign of the strange-quark chemical potential to be an experimentally accessible order parameter and a unique, concise and well-defined indication of the quark-deconfinement phase transition in nuclear matter.

PACS numbers: 25.75.+r, 12.38.Mh, 24.84.+p

1. Introduction

It is generally expected that ultra-relativistic nucleus-nucleus collisions will provide the basis for strong interaction thermodynamics, which will lead to new physics. Quantum Chromodynamics for massless quarks free of dimensional scales contain the intrinsic potential for the spontaneous generation of two scales: one for the confinement force, coupling quarks to form hadrons and one for the chiral force, binding the collective excitations to Goldstone bosons. In thermodynamics, these two scales lead to two possible consecutive phase transitions, deconfinement and chiral symmetry restoration, characterized by corresponding critical temperatures: T_d and T_χ , [1]. At temperatures above T_d , hadrons dissolve into quarks and gluons, whereas at T_χ , chiral symmetry is fully restored and quarks become almost massless (assuming that a thermal mass is acquired for $T > T_d$), forming the Quark - Gluon Plasma (QGP). A priori it is not evident that both non-perturbative transitions have to take place at the same temperature. At finite net baryon number density, $T_d < T_\chi$ would correspond to a regime of unbound, massive, correlated and interacting, 'constituent-like' quarks [2], as they

appear in the additive quark model for hadron-hadron and hadron-lepton interactions [3]. Thus, the consecutive appearance of these two transitions, deconfinement and chiral symmetry restoration, forms an intermediate region on the phase diagram, the Deconfined Quark Matter (DQM), in-between the Hadron Gas (HG) and the chiral QGP domains. Therefore, we define a QCD phase diagram of strongly interacting matter at finite baryon number density with three regions: HG - DQM - QGP [4-6].

The necessity for such an intermediate region with interacting quarks and gluons is conjectured also from recent lattice calculations [7], which show that $\varepsilon(2T_d) \sim 0.85\varepsilon_{SB}$ and $3P(2T_d) \sim 0.66\varepsilon_{SB}$, where ε_{SB} is the Stefan-Boltzmann ideal QGP value for the energy density. In addition, the running coupling constant has a value $\alpha_s(T \sim 300\text{MeV}) \sim 0.3$, indicating substantial strong interaction even at this high temperature. These observations substantiate quantitatively the need for an intermediate domain with $1 > \alpha_s > 0$, where massive and correlated-interacting quarks are found. This domain does not have a defined upper border, but goes asymptotically into the chirally symmetric QGP region with increasing temperature and quark chemical potential. At zero baryon density, $T_d = T_\chi = T_0(\mu_q = 0)$, and the DQM domain vanishes.

Such a 3-state phase diagramme could be described by the variation of thermodynamic quantities from one region to the other. The task is to establish a well-defined quantity, which changes concisely (and measurably) as nuclear matter changes phases, thus indicating deconfinement and / or chiral symmetry restoration. If this quantity can be expressed in a functional form of other thermodynamic parameters (for example the temperature) within an Equation of State (EoS), one may then describe accurately its variation throughout the phase diagramme and employ it as an order parameter. We propose and show that the equilibrated strange-quark chemical potential of the strongly interacting system is the sought-for thermodynamic quantity. This suggestion was firstly put forth earlier in [5].

In sections 2, 3 and 4 we discuss the partition functions for the strange hadron sector in the HG, chiral QGP and DQM phases, respectively. Taking into account in an approximate way the dynamics of the DQM phase, we construct an empirical Equation of State for this domain. We employ it, together with the known EoS of the HG and QGP phases, to obtain the strange-quark chemical potential in a functional form of the temperature and light-quark chemical potential throughout the phase diagram. With this relation we study the variation of μ_s , attributing the changes in the sign and magnitude of the strange-quark chemical potential to the changes of phase of nuclear matter. In section 5 we summarize several thermal model analyses of experimental particle yield data from nucleus-nucleus interactions at AGS and SPS. Among the latter, the S+A interactions at 200 AGeV may be characterized by the existence of negative strange-quark chemical potential. In section 6 we predict the values for certain strange particle ratios and suggest experiments at RHIC at lower energies, where the baryon number density is finite. Finally, in section 7 we discuss our proposals and come to conclusions whether the S+A and Pb+Pb interactions at the SPS have entered the deconfined phase.

2. Hadron Gas phase

In the HG phase, the mass spectrum is given in the Boltzmann approximation by the partition function, $\ln Z_{HG}$. We assume that the hadronic state has attained thermal and chemical equilibration of three quark flavors (u, d, s):

$$\begin{aligned} \ln Z_{HG}(T, V, \lambda_q, \lambda_s) = & Z_m + Z_n(\lambda_q^3 + \lambda_q^{-3}) + Z_K(\lambda_q \lambda_s^{-1} + \lambda_q^{-1} \lambda_s) + Z_Y(\lambda_q^2 \lambda_s + \lambda_q^{-2} \lambda_s^{-1}) \\ & + Z_{\Xi}(\lambda_q \lambda_s^2 + \lambda_q^{-1} \lambda_s^{-2}) + Z_{\Omega}(\lambda_s^3 + \lambda_s^{-3}) \quad (q = u, d) \quad (1) \end{aligned}$$

The one particle Boltzmann partition function Z_k is given by

$$Z_k(V, T) = \frac{VT^3}{2\pi^2} \sum_j g_j \left(\frac{m_j}{T}\right)^2 K_2\left(\frac{m_j}{T}\right)$$

The fugacity λ_i^k controls the quark content of the k-hadron, i = s, b for strangeness and baryon number [$\lambda_b = \lambda_q^3 = e^{3\mu_q/T}$], respectively. The summation in Eq. (2) runs over the resonances of each hadron species with mass m_j , and the degeneracy factor g_j counts the spin and isospin degrees of freedom of the j-resonance. For the strange hadron sector, kaons with masses up to 2045 MeV/c², hyperons up to 2350 MeV/c² and cascades up to 2025 MeV/c² are included, as well as the known Ω -states at 1672 MeV and 2252 MeV. For simplicity, we assume isospin symmetry in Eq. (1), $\mu_u = \mu_d = \mu_q$. Strangeness neutrality in strong interactions necessitates:

$$\langle N_s - N_{\bar{s}} \rangle = \frac{T}{V} \frac{\partial}{\partial \mu_s} \ln Z_{HG}(T, V, \lambda_q, \lambda_s) = 0 \quad (2)$$

which reduces to

$$Z_K(\lambda_q^{-1} \lambda_s - \lambda_q \lambda_s^{-1}) + Z_Y(\lambda_q^2 \lambda_s - \lambda_q^{-2} \lambda_s^{-1}) + 2Z_{\Xi}(\lambda_q \lambda_s^2 - \lambda_q^{-1} \lambda_s^{-2}) + 3Z_{\Omega}(\lambda_s^3 - \lambda_s^{-3}) = 0 \quad (3)$$

This is an important condition as it defines the relation between light- and strange-quark fugacities in the equilibrated primordial state. Eq. (4) can be used to derive the true (transverse-flow independent) temperature of the state, once the fugacities λ_q and λ_s are known from experimental strange particle yield ratios [4].

In the HG phase with finite net baryon number density, the chemical potentials μ_q and μ_s are coupled through the production of strange hadrons. Due to this coupling, strangeness conservation does not necessitate $\mu_s = 0$ everywhere in this phase. In fact, $\mu_s > 0$ in the hadronic domain. The condition $\mu_s = 0$ requires $\lambda_s = \lambda_s^{-1} = 1$, and Eq. (4) becomes [8],

$$\left[Z_Y(\lambda_q + \lambda_q^{-1}) - Z_K + 2Z_{\Xi} \right] (\lambda_q - \lambda_q^{-1}) = 0$$

The first factor gives the curve μ_q as a function of T in the phase diagram, along which $\mu_s = 0$:

$$\mu_q(T) = T \cosh^{-1} \left(\frac{Z_K}{2Z_Y} - \frac{Z_{\Xi}}{Z_Y} \right) \quad (4)$$

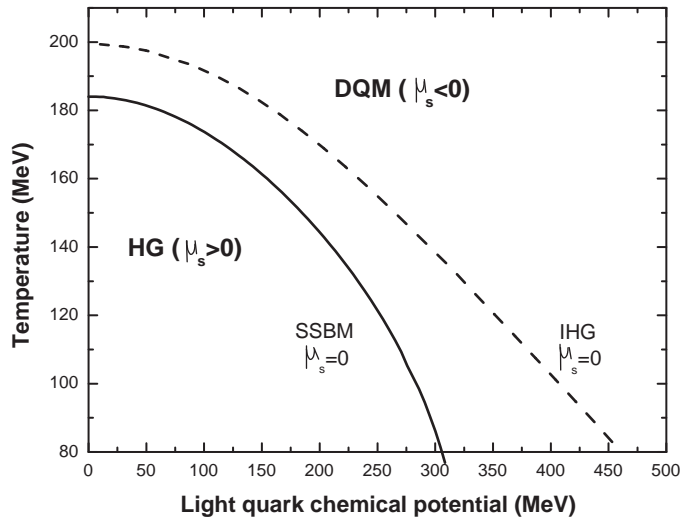


Figure 1. The hadronic boundary within the SSBM and IHG models. The IHG $\mu_s = 0$ line lies higher than the SSBM one.

A more elegant and concise formalism describing the HG phase is the Strangeness-including Statistical Bootstrap model (SSBM) [9]. It includes the hadronic interactions through the mass spectrum of all hadron species, in contrast to all other ideal hadron gas formalisms. The SSBM is valid and applicable only within the hadronic phase, defining in a determined way the limits of this phase. The boundary of the hadronic domain is given by the projection on the 2-dimensional (T, μ_q) phase diagram of the intersection of the 3-dimensional bootstrap surface with the strangeness-neutrality surface ($\mu_s = 0$). Note that the vanishing of the strange-quark chemical potential on the HG borderline does not apriori suggest that $\mu_s = 0$ everywhere beyond this phase. It only states that $\mu_s = 0$ characterizes the end of the hadronic phase. According to this definition of the HG boundary, we consider the hadronic phase, described by Eq. (4) in the ideal HG model, to be terminated at the line where the strange quark chemical potential vanishes, despite the fact that Eq. (4) maps the hadronic domain independently of the value of μ_s . That is, in the ideal HG model we consider the upper limit of the hadronic phase to be defined by Eq. (5). The relative position of the two boundaries for the hadron gas domain on the phase diagram, as defined by the two models, is shown in Fig. 1. We note that the ideal HG boundary lies about 15 MeV higher than the SSBM one (for $\mu_q < 100 \text{ MeV}$), due to the absence of interactions in the former.

3. Chirally symmetric QGP phase

In the chirally symmetric QGP region, the partition function for the current-mass u, d, s-quarks and gluons has the form:

$$\ln Z_{QGP}(T, V, \mu_q, \mu_s) = \frac{V}{T} \left[\frac{37}{90} \pi^2 T^4 + \mu_q^2 T^2 + \frac{\mu_q^4}{2\pi^2} + \frac{g_s m_s^0{}^2 T^2}{2\pi^2} (\lambda_s + \lambda_s^{-1}) K_2 \left(\frac{m_s^0}{T} \right) \right] \quad (5)$$

where m_s^0 and g_s is the current-mass and degeneracy of the s-quark, respectively. Strangeness conservation gives $\lambda_s = \lambda_s^{-1} = 1$, or

$$\mu_s^{QGP}(T, \mu_q) = 0 \quad (6)$$

throughout this phase. Here the two order parameters, the average thermal Wilson loop $\langle L \rangle$ and the scalar quark density $\langle \bar{\psi}\psi \rangle$, have reached their asymptotic values. Note that the chirally symmetric quark-gluon plasma phase always corresponds to a vanishing strange quark chemical potential, even if we take into account perturbative corrections to the partition function of Eq. (6). Thus, the chiral symmetry restoration critical temperature T_χ is not associated with the fact that we consider, for simplicity, an ideal quark-gluon gas to describe the QGP.

4. Deconfined Quark Matter Phase (DQM)

In formulating our description beyond the hadronic phase, we use the following picture: The thermally and chemically equilibrated primordial state at finite baryon number density, produced in nucleus-nucleus interactions, consists of the deconfined valance quarks of the participant nucleons, as well as of $q - \bar{q}$ pairs ($q=u,d,s$), created by quark and gluon interactions. Beyond but near the HG boundary, $T \geq T_d$, the correlation-interaction between $q - q$ is near maximum, $\alpha_s(T) \leq 1$, a prelude to confinement into hadrons upon hadronization. With increasing temperature, the correlation-interaction of the deconfined quarks gradually weakens, $\alpha_s(T) \rightarrow 0$, as colour mobility and colour charge screening increase. The mass of all (anti)quarks depend on the temperature and scale according to a prescribed way. The initially constituent mass decreases with increasing T, and as the DQM region goes asymptotically into the chirally symmetric QGP domain, as $T \rightarrow T_\chi$, quarks attain current mass. In this formulation, the equation of state in the DQM region should lead to the EoS of the hadronic phase, Eq. (1), at $T < T_d$, and to the EoS of the QGP, Eq. (6), at $T \sim T_\chi$.

To construct the empirical EoS in the DQM phase, we use the two order parameters (for details see Appendix A):

- (i) Average thermal Wilson loop, $\langle L \rangle = e^{-F_q/T} \sim R_d(T) = 0 \rightarrow 1$, as $T = T_d \rightarrow T_\chi$, describing the quark deconfinement and subsequent colour mobility, F_q being the free quark energy.
- (ii) Scalar quark density, $\langle \bar{\psi}\psi \rangle \sim R_\chi(T) = 1 \rightarrow 0$, as $T = T_d \rightarrow T_\chi$, denoting the scaling of the quark mass with temperature.

Although the Wilson-Polyakov loop is not yet calculated for a finite density system, we consider that, in the case of non zero baryochemical potential, it has a smooth temperature dependence, as suggested in [10[†],11], attaining non-limiting values for a range of temperatures and, therefore, implying the broadening of the transition region. This permits us to approximate the order parameter for the finite baryon density case with an arbitrary, general, yet non-step functional form.

4.1. Definition of the order parameters

In order to construct the EoS in the DQM region it is necessary to employ an analytic functional form of the order parameters. We have approximated the Wilson loop, obtained from zero density lattice calculations, with two different functions of temperature and chemical potential:

$$R_d(T) = \begin{cases} \Theta(T - T_d), & \mu_q = 0 \\ \frac{1}{1 + \exp[-\alpha(T - \beta)]}, & \mu_q > 0 \end{cases} \quad (7)$$

and

$$R_d(T) = \begin{cases} \Theta(T - T_d), & \mu_q = 0 \\ c \left(\frac{T - T_d}{T} \right)^\nu, & \mu_q > 0 \end{cases} \quad (8)$$

In Eq. (7) a Fermi-type function is used for finite μ_q , where the parameters $\{\alpha, \beta\}$ control the difference of the critical temperatures T_d and T_χ , i.e., when $R_d \sim 0$ and $R_d \sim 1$, respectively. They can be chosen arbitrarily in order to obtain realistic compatibility with the lattice QCD results. In Eq. (8) the order parameter is described using a more common, in the theory of critical phenomena, function near the critical point T_d , where the critical exponent ν can be chosen according to universality class arguments or arbitrarily. The parameter c simply controls the values of $R_d(T)$, so that asymptotically $R_d(T) \rightarrow 1$ as $T \rightarrow T_\chi$. Note that the exact expression for the considered order parameter $R_d(T)$ is not of crucial importance for this qualitative description (see Appendix A). Figures 2, 3 show the approximated order parameter for different values of $\{\alpha, \beta\}$ and of the critical exponent ν , respectively, for the finite chemical potential case, $\mu_q > 0$. In Figure 4 we show the two approximated order parameters, where for simplicity we have taken $R_\chi(T) \equiv 1 - R_d(T)$ and used Eq. (8) with the parameterization $\{\alpha = 0.03, \beta = 268\}$.

4.2. The DQM Equation of State

We assume that above T_d the deconfined quarks retain a degree of correlation, resembling "hadron-like" states, since $1 > \alpha_s(T) > 0$. The diminishing of this correlation-interaction, as a result of progressive increase of colour mobility, is approximated by the

[†] These finite baryon density simulations use a canonical partition function and have provided results in the quenched (heavy quark mass) limit of QCD within the presence of static quarks.

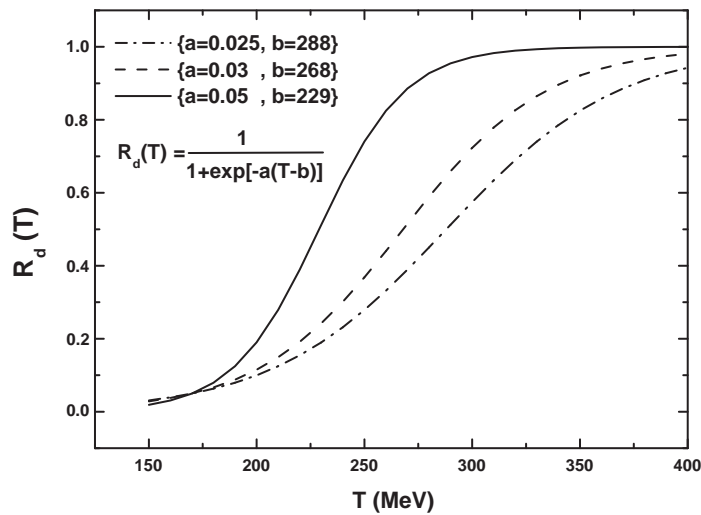


Figure 2. Approximated finite density Polyakov loop $R_d(T)$, obtained from Eq.(8) for different values of the model parameters $\{\alpha, \beta\}$.

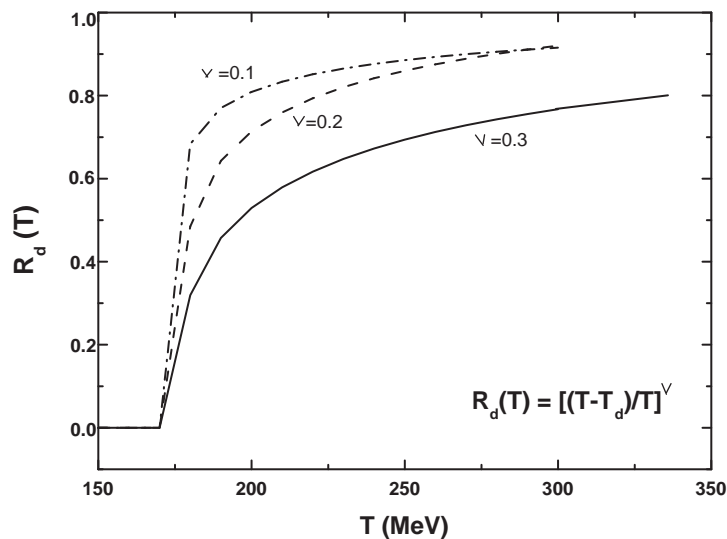


Figure 3. Approximated finite density Polyakov loop $R_d(T)$, obtained from Eq.(9) for different values of the model parameter ν .

factor: $[1 - R_d(T)] = 1 \rightarrow 0$, as $T = T_d \rightarrow T_\chi$. Note that effectively $[1 - R_d(T)] \sim \alpha_s(T)$ in the DQM region, the temperature dependence of the running coupling constant [12]. To account for the "effective mass" of the state as a function of temperature, we assume the mass of the quarks to decrease from the constituent value and reach the current-mass

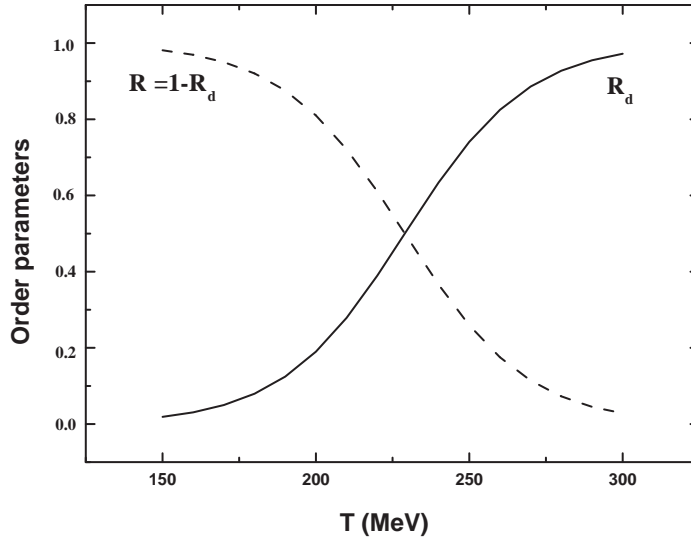


Figure 4. Plot of the approximated order parameters $R_d(T)$ and $R_\chi(T) = 1 - R_d(T)$ using Eq.(7) with $\alpha = 0.03$ and $\beta = 268$.

as $T \rightarrow T_\chi$. The quark mass scales with temperature as:

$$m_q^*(T) = R_\chi(T)(m_q - m_q^0) + m_q^0 \quad (9)$$

where m_q and m_q^0 are the constituent and current quark masses, respectively, ($m_u^0 \sim 5 \text{ MeV}$, $m_d^0 \sim 9 \text{ MeV}$, $m_s^0 \sim 170 \text{ MeV}$). Similarly, the effective hadron-like mass scales as:

$$m_i^*(T) = R_\chi(T)(m_i - m_i^0) + m_i^0 \quad (10)$$

where m_i is the hadron mass in the hadronic phase and m_i^0 is equal to the sum of the hadron's quarks current-mass ($m_K^0 \sim 175 \text{ MeV}$, $m_Y^0 \sim 185 \text{ MeV}$, $m_X^0 \sim 350 \text{ MeV}$ and $m_Q^0 \sim 510 \text{ MeV}$). In the EOS, the former scaling is employed in the mass-scaled partition function $\ln Z_{QGP}^*$, whereas the latter in the mass-scaled partition function $\ln Z_{HG}^*$, which accounts for the produced hadron species. Note that this mass-scaling is effectively equivalent to the one given in the Nambu - Jona-Lasinio (NJL) formalism [13] (see Appendix B).

Employing the described dynamics, we construct an empirical partition function of the DQM phase:

$$\ln Z_{DQM}(V, T, \lambda_q, \lambda_s) = [1 - R_d(T)] \ln Z_{HG}^*(V, T, \lambda_q, \lambda_s) + R_d(T) \ln Z_{QGP}^*(V, T, \lambda_q, \lambda_s) \quad (11)$$

The proposed intermediate DQM phase should not be confused with a mixed hadronic-partonic phase. The partition function of Eq. (11) is written as a linear combination of the HG and QGP mass-scaled partition functions. It is a realistic and convenient approximation, which satisfies the general property of the partition function, describing

asymptotically confinement and chiral symmetry restoration. In the intermediate temperature regime of the DQM phase, neither pure hadronic bound states, nor chirally symmetric QGP clusters can be found. In Eq. (11) the factor $[1 - R_d(T)]$ describes the weakening of the correlation-interaction of the deconfined quarks constituting the "hadron-like" entities and gives the mass-scaling of these entities with increasing temperature. In the second term, the factor $R_d(T)$ defines the rate of colour mobility, whereas $\ln Z_{QGP}^*$ represents the state as it approaches the QGP region. Thus, at $T = T_d$, the EoS of the DQM region goes over to the corresponding in the HG phase and at $T \sim T_\chi$, to the EoS in the chirally symmetric QGP region.

Strangeness neutrality in the DQM phase leads to the EoS:

$$[1 - R_d(T)] \left[Z_K^*(\lambda_s \lambda_q^{-1} - \lambda_q \lambda_s^{-1}) + Z_Y^*(\lambda_s \lambda_q^2 - \lambda_s^{-1} \lambda_q^{-2}) + 2Z_\Xi^*(\lambda_s^2 \lambda_q - \lambda_s^{-2} \lambda_q^{-1}) + 3Z_\Omega^*(\lambda_s^3 - \lambda_s^{-3}) \right] + R_d(T) g_s m_s^{*2} K_2 \left(\frac{m_s^*}{T} \right) (\lambda_s - \lambda_s^{-1}) = 0 \quad (12)$$

For given μ_q , Eq. (12) defines the variation of the strange-quark chemical potential with temperature in the DQM domain. Combining Eq's (4, 12) we obtain the change of the strange-quark chemical potential with temperature in the entire phase diagram.

4.3. Zero chemical potential, $\mu_q = 0$

In the case of vanishing baryon chemical potential, quarks attain current mass instantaneously upon deconfinement, due to the fact that $R_\chi(T)$ becomes a step function with $R_\chi(T, \mu_q = 0) = 0$, for temperatures $T > T_d$, Eq's (7), (8). Consequently, the chirally symmetric QGP phase follows immediately after the HG phase, as can be seen from Eq. (12) and the partition function beyond the HG region is given by Eq. (6). The deconfinement and chiral symmetry transitions coincide, $T_d = T$, and the DQM phase with negative strange-quark chemical potential vanishes. Due to vanishing baryon chemical potential, the EoS (12) leads to $\mu_s = 0$ for all temperatures. In this case, the strange-quark chemical potential cannot provide a signal for any phase transition. Figure 5 exhibits this effect, showing the variation of μ_s with temperature for different values of the light-quark chemical potential μ_q .

4.4. Finite chemical potential, $\mu_q > 0$

The situation for a non-vanishing baryon chemical potential is not yet known in terms of lattice calculations. Within this model we can easily extend our analysis for a system of finite and fixed μ_q according to Eq. (12). In Fig. 6 the strange-quark chemical potential maps the QCD phase diagram as a function of T , for $\mu_q/T = 0.45$. We observe that μ_s attains positive values in the HG phase, as a result of the coupling between μ_q and μ_s in strange hadrons. It approaches zero as the hadron density reaches its asymptotic Hagedorn limit at the end of the hadronic phase, where a phase transition to partonic matter takes place, at the deconfinement temperature T_d [14]. At this temperature, $\mu_s(T_d) = 0$, signifying the vanishing of this coupling in hadrons. In the

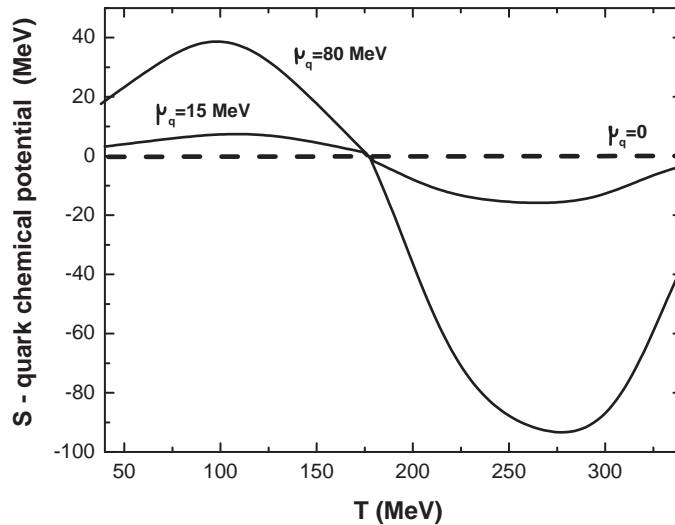


Figure 5. Variation of μ_s with T for various values of μ_q . For zero μ_q , μ_s vanishes for all temperatures.

DQM region it grows strongly negative, where an effective correlation - progressively weakening - remains in effect among the deconfined, but interacting quarks with non-current mass. Finally μ_s returns to zero as the QGP phase is approached, with restored chiral symmetry (current-mass quarks) and α_s approaching zero.

Figure 7 exhibits the variation of μ_s/T as a function of T throughout the 3-region phase diagram for $\mu_q = 0.45T$. We have assumed that the deconfinement temperature is $T_d \sim 176 \text{ MeV}$ at $\mu_q \sim 80 \text{ MeV}$, as given by the SSBM hadronic phase boundary [15]. We observe that:

a) If the deconfined-quark mass were to attain its current value ($m_q = m_q^0$) beyond T_d , then μ_s would be zero for $T > T_d$, curve (a).

b) If $0 < R_d < 1$ and $m_q^0 < m_q^*(T) < m_q$, then the EoS (12), which includes mass-scaled "hadron-like" states, as well as (anti)quarks with scaled mass, gives large negative values for μ_s/T in the DQM phase. After reaching a minimum, μ_s/T returns asymptotically to zero as the QGP phase is approached at $T_\chi \sim (2 - 4)T_d$, depending in general on μ_q , Fig. 7, curve (b).

c) Scaling alone of the effective hadron masses produces large negative strange-quark chemical potential beyond the HG phase, saturating at high temperature without ever returning to zero at the QGP phase, Fig. 7, curve (c).

The fact that we obtain a chiral symmetry restoration temperature $T_\chi \sim (2 - 4)T_d$ for $\mu_q \sim 80 \text{ MeV}$, is a result of the specific parameterization used for the order parameter. The DQM phase exists for $0 < R_d < 1$, so it is actually the condition $R_d(T_\chi) = 1$ that determines the end of DQM at $T \rightarrow T_\chi$. In general, $T_\chi = k(\mu_q)T_d$, where $k(\mu_q > 0) > 1$ and $k(\mu_q = 0) = 1$. However, finite baryon chemical potential

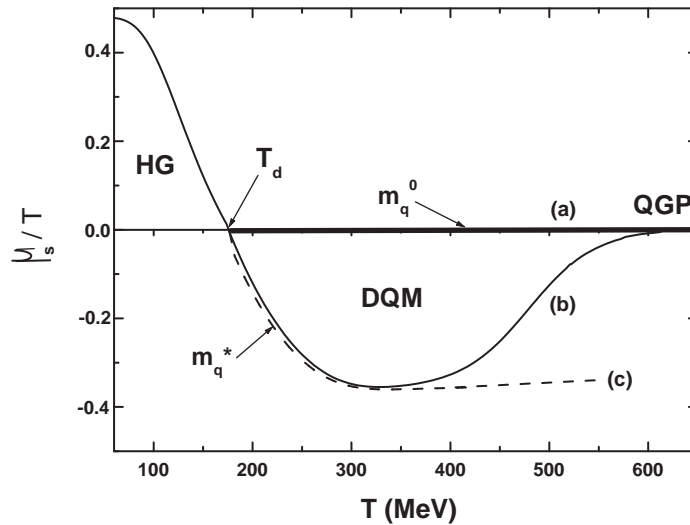


Figure 7. Variation of μ_s/T with temperature in the DQM region for different considerations of the parameters of the EoS, eq. (12).

will be always associated with the existence of negative μ_s and therefore $T_\chi > T_d$, meaning that the two phase transitions, deconfinement and chiral, are apart. This is an interesting result, which is connected with the existence of negative strange-quark chemical potential. Note that there is no known argument from QCD that the two transitions occur at the same temperature for finite baryon density.

On the basis of the above observations, we propose that the change in the sign of the strange-quark chemical potential, from positive in the HG phase to negative in the DQM, defines uniquely and precisely the phase transition to quark-deconfinement at finite baryon density. The experimental observation of negative μ_s would be an evidence for the existence of the DQM region and consequently of the fact that chiral symmetry restoration follows deconfinement ($T_d < T_\chi$). We note that the sign of μ_s , positive in the HG, negative in the DQM and zero in the QGP domains, is independent of the particular form of the parameters R_d and R_χ used in the EoS and unique in each region (see Appendix A). It can be considered and used as a potentially experimentally accessible order parameter of the deconfinement phase transition. This signature is independent of assumptions and ambiguities regarding interaction mechanisms and matter media effects, as well as weakness and uncertainties in the predictive power of models, as is the case with other proposed signs for deconfinement: J/ψ suppression, resonance shift and broadening, strangeness enhancement, etc. In the present calculation, however, the magnitude and shape of the negative chemical potential curve as a function of temperature should be taken in a qualitative manner, due to the empirical treatment of the dynamics in the DQM phase. A detailed, quantitative treatment of the DQM EoS will require the use of a three-flavor effective Lagrangian in the NJL formalism [16].

5. Experimental Data

Data from nucleus-nucleus interactions, obtained by experiments E802 [17] at AGS and NA35 [18], NA49 [19] at SPS have been analyzed in terms of several statistical-thermal models: the Strangeness-including Statistical Bootstrap Model, SSBM [9, 15, 20-22] and others employing the canonical and grand-canonical formalisms [23-27]. The data analysis is made, of course, within the inevitable limitations of all thermal-statistical models and the assumption of a thermalized and equilibrated matter. There are proposals for possible non-equilibrium effects, however thermal models seem to be in surprisingly well consistency with the experimental data. Table 1 summarizes the results of these analyses, from which the quantities T , μ_q and μ_s have been deduced. Observe that all interactions, studied so far, exhibit positive μ_s and therefore there does not yet exist a confident experimental confirmation of negative values for the strange-quark chemical potential. Note that in [23,25,26] the negative μ_S refers to the strangeness chemical potential, which is related to the strange-quark chemical potential by: $\mu_S = \mu_s + \mu_q$. This fact led to a misinterpretation in [28]. However the sulfur-induced interactions may deserve a more cautious examination, as suggested by the SSBM analysis. In contrast to other thermal-statistical models, the Statistical Bootstrap Model (SBM) of Hagedorn [29] incorporates the hadronic interactions in the EoS through the bootstrap equation. The development of the SBM with the inclusion of Strangeness (SSBM) has been employed in the analysis of nucleus-nucleus interactions at the SPS. The SSBM analysis for the S+S interaction [15] has shown that this equilibrated state is situated mostly (75%) outside the hadronic phase, whereas the S+Ag [21] is just on the deconfinement line. In addition, the calculations have pointed out a large ($\sim 30\%$) entropy enhancement of the experimental data compared to the model, an effect observed also by other calculations [23-25]. This enhancement may be attributed to contributions from the DQM phase with many liberated new partonic degrees of freedom.

The fact that beyond the HG phase the deconfined quarks retain a degree of correlation, resembling "hadron-like" states, allows the thermal models [23-25] to describe the state adequately using a hadron gas EoS. These models do not sense the HG phase limit and treat the deconfined state as consisting of colorless hadrons. However, an ideal Hadron Gas model with no interactions exhibits strong deviations from the SSBM as we approach the critical region ($T \sim 175 \text{ MeV}$), where the sulfur-induced interactions are approximately situated. Within the IHG model the condition $\mu_s = 0$ is satisfied for a higher temperature $T_0 \sim 200 \text{ MeV}$, extending the HG phase to a larger region in the phase diagram (see Fig. 1). Consequently, the negative strange-quark chemical potential, a characteristic of the region beyond the HG phase, appears at higher temperatures also for the ideal HG model, Fig. 8. This is the reason why $\mu_s > 0$ in the analysis of [23, 25], although a temperature above the deconfinement (according to the SSBM) is obtained. If the IHG curve is shifted in a way that would approximate the SSBM boundary, then negative μ_s should be obtained for the S+A

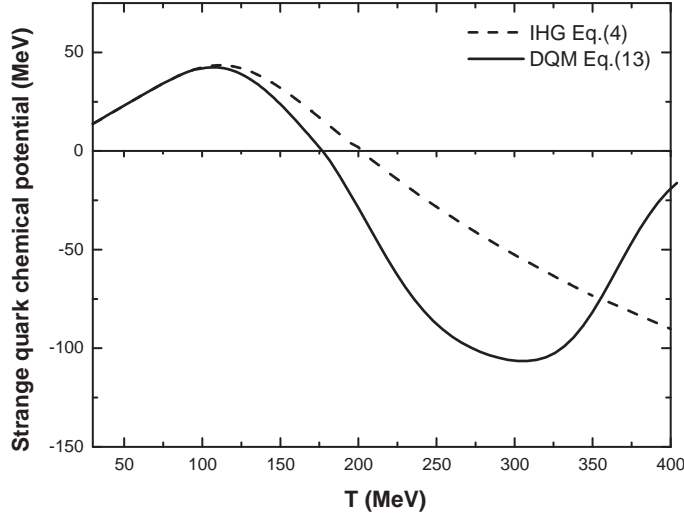


Figure 8. Variation of the strange quark chemical potential with the temperature within the IHG formalism and the proposed DQM. The change in the sign of μ_s is realized at a higher temperature for the IHG model.

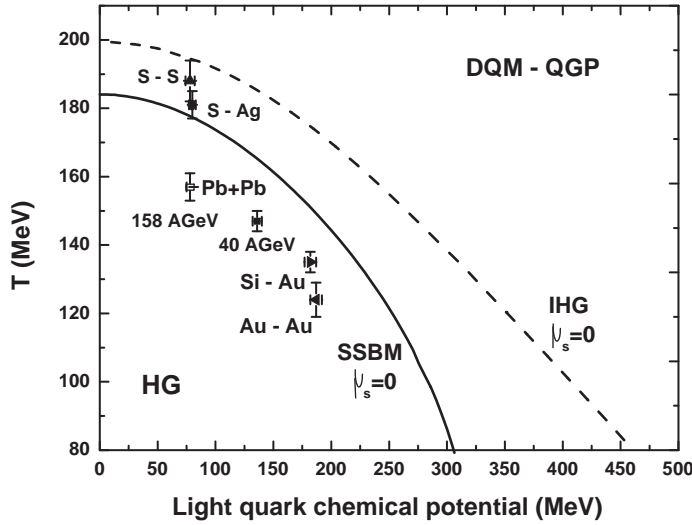


Figure 9. Phase diagram with the SSBM deconfinement line and the location (T, μ_q average values) of several interactions, deduced from the analysis with thermal models.

interactions. Note that this effect is not important in the study of the other A+A interactions, because in their case the equilibrated states are situated far below the critical temperature and therefore the HG model is very close to the analysis by the SSBM. This can be seen in Table 1, where the analysis of the experimental data within the two models is almost identical for extracted temperatures below 160 MeV. For the $Pb + Pb$ interaction, the SSBM analysis [22] has shown the system to be located well

Table 1. Deduced values for T , μ_q , μ_s from several thermal models and fits to experimental data for several interactions.

Interaction/Experiment				
Si+Au(14.6 AGeV)/E802				
	Reference[28]	Reference[26]	Mean	
T(MeV)	134±6	135±4	135±3	
μ_q (MeV)	176±12	194±11	182±5	
μ_s (MeV)	66±10		66±10	
Au+Au(11.6 AGeV)/E802				
	Reference[28]	Reference[26]	Mean	
T(MeV)	144±12	121±54	124±5	
μ_q (MeV)	193±17	186±5	187±5	
μ_s (MeV)	51±14		51±14	
Pb+Pb(158 AGeV)/NA49				
	Reference[28]	Reference[26]	Reference[22]	Mean
T(MeV)	146±9	158±3	157±4	157±3
μ_q (MeV)	74±6	79±4	81±7	78±3
μ_s (MeV)	22±3		25±4	23±2
Pb+Pb(40 AGeV)/NA49*				
	Reference[28]	Reference[32]	Mean	
T(MeV)	147±3	150±8	149±9	
μ_q (MeV)	136±4	132±7	134±8	
μ_s (MeV)	35±4			
S+S(200 AGeV)/NA35				
	Reference[23]	Reference[25]	Reference[24]	Mean
T(MeV)	182±9	181±11	202±13	188±6
μ_q (MeV)	75±6	73±7	87±7	78±4
μ_s (MeV)	14±4	17±6		16±7
S+Ag(200 AGeV)/NA35				
	Reference[23]	Reference[25]	Reference[24]	Mean
T(MeV)	180±3	179±8	185±8	181±4
μ_q (MeV)	79±4	81±6	81±7	80±3
μ_s (MeV)	14±4	16±5		16±8

*NA49 private communication

within the hadronic phase. In addition, thermal model calculations [22, 26] find no entropy enhancement for this interaction. Figure 9 shows the 3-flavor phase diagram with the SSBM maximally extended \ddagger deconfinement line, the IHG $\mu_s = 0$ line and the location of the state (T , μ_q mean values) for several interactions, Table 1. Observe that the sulfur-induced interactions at 200 AGeV, are situated beyond the SSBM deconfinement line, whereas all others are well within the hadronic phase.

\ddagger The maximally extended HG phase limit is defined for $T_0(\mu_q = 0) \sim 183$ MeV, which is the maximum temperature for non-negative μ_s in the HG domain. Recent lattice QCD calculations give $T_0 \sim 175$ MeV for [2+1] quark flavors [7].

6. Predictions for particle yield ratios at RHIC

New data obtained at RHIC with the $Au + Au$ interaction at $\sqrt{s} = 130 \text{ AGeV}$ (see a compilation of data in [30]) show that at midrapidity the light quark fugacity is $\lambda_q \sim 1.08$, indicating very small quark chemical potential. This has an effect on the strange-quark chemical potential, making it close to zero throughout the 3-region phase diagram (see Fig. 5). In such case of minimal net baryon density, our model cannot be applied, as discussed in Section 4.3. We have, therefore, calculated the particle yield ratios Ω^+/Ω^- and Ξ^+/Ξ^- for finite baryon density, obtained in $Au + Au$ interactions at $\sqrt{s} = 20 - 90 \text{ AGeV}$. The quantities needed for these calculations, μ_q/T and T of the equilibrated state, were obtained by fitting all available corresponding values, obtained for equilibrated states in nucleus-nucleus collisions from SIS to SPS [26, 27] and extrapolating to RHIC energies. The data were fitted as a function of $(\sqrt{s}/\text{participant})$. Figures 10, 11 show the fitted temperatures and μ_q/T and their

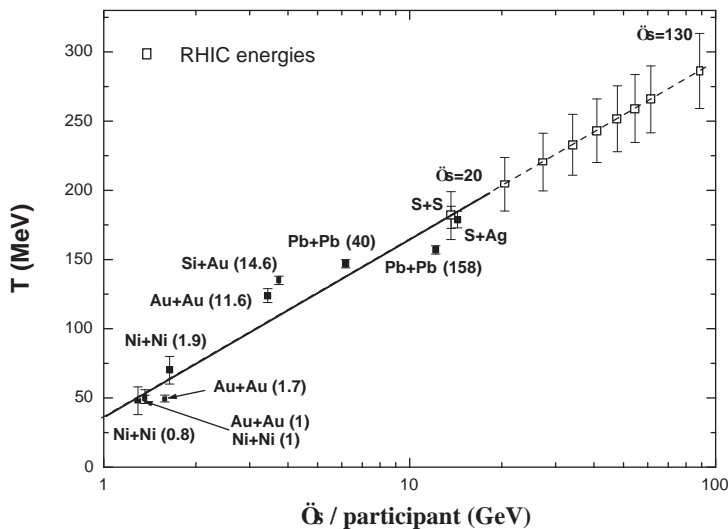


Figure 10. Fitted temperatures as a function of $(\sqrt{s}/\text{participant})$ and extrapolation to RHIC energies $20 < \sqrt{s} < 130 \text{ AGeV}$. The energy in parenthesis is in units of AGeV.

extrapolation to higher energies, respectively. Table 2 contains the extrapolated values for T and μ_q/T , corresponding to equilibrated primordial states (not chemical freeze out), as well as the order of magnitude predictions of our empirical EoS in DQM for μ_s/T and for the two particle ratios, for two different R_d curves. A worth mentioning result of the extrapolation is that, at $\sqrt{s} = 130 \text{ AGeV}$, a primordial fireball temperature $T \sim O(280 \text{ MeV})$ is found, which is much higher than the freeze out temperature $T \sim 175 \text{ MeV}$, obtained in [30]. It may be that in the region of minimal baryon chemical potential, the hadronization process of a deconfined state is continuous and smooth and thus the primordial thermodynamic quantities are not conserved. It should also be kept in mind that the available RHIC data span a very small rapidity range

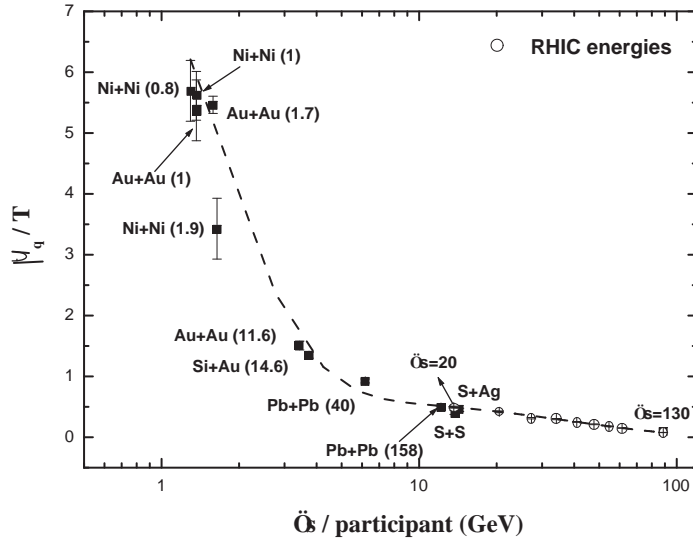


Figure 11. Fit to the μ_q/T values of several interactions and extrapolation to RHIC energies $20 < \sqrt{s} < 130 \text{ AGeV}$. The energy in parenthesis is in units of AGeV.

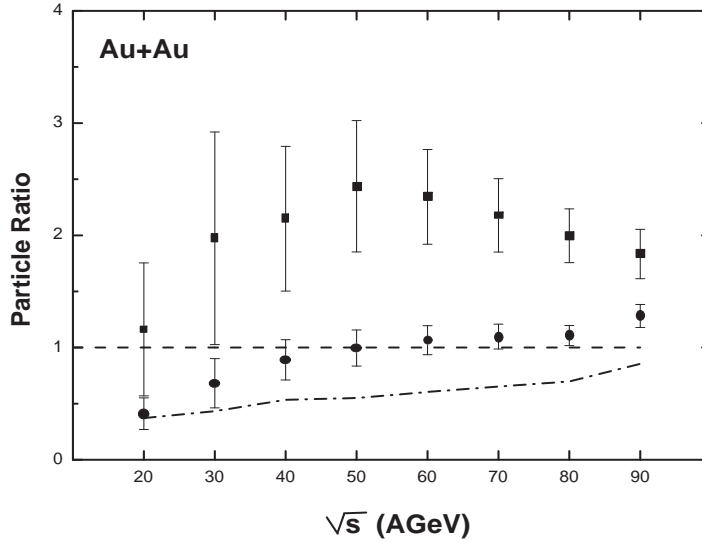


Figure 12. Predicted particle yield ratios Ω^+/Ω^- [■] and Ξ^+/Ξ^- [●] for a finite baryon density region, obtained in $Au + Au$ interactions at $\sqrt{s} = 20 - 90 \text{ AGeV}$. The lines correspond to the case $\mu_s = 0$ for the ratio Ω^+/Ω^- [---] and Ξ^+/Ξ^- [- · - ·].

($\Delta y < \pm 1$), making unreliable the extraction of values for global thermodynamic quantities from these fits. Figure 12 shows the range of the predicted particle ratios and the maximum values of the ratios in the case where μ_s does not become negative, but stays zero after deconfinement. Note that negative μ_s means that the particle yield

Table 2. The extrapolated values for the temperature T and the ratio μ_q/T obtained for the Au+Au interaction at RHIC, as well as predictions of the empirical EoS for μ_s/T and two strange-particle ratios. Table (a) exhibits the results for $\{\alpha = 0.03, \beta = 268\}$ and (b) for $\{\alpha = 0.05, \beta = 229\}$ in Eq. (7).

(a)					
$\sqrt{s}(A\text{GeV})$	$T(\text{MeV})$	μ_q/T	μ_s/T	Ω^+/Ω^-	Ξ^+/Ξ^-
20	181.76 \pm 17.30	0.49 \pm 0.02	-0.03 \pm 0.17	1.20 \pm 1.22	0.42 \pm 0.28
30	204.40 \pm 19.35	0.42 \pm 0.01	-0.20 \pm 0.10	3.24 \pm 1.94	0.95 \pm 0.38
40	220.45 \pm 20.85	0.31 \pm 0.01	-0.21 \pm 0.05	3.50 \pm 1.05	1.23 \pm 0.25
50	232.91 \pm 22.02	0.30 \pm 0.01	-0.22 \pm 0.05	3.77 \pm 1.13	1.33 \pm 0.27
60	243.10 \pm 23.06	0.25 \pm 0.01	-0.19 \pm 0.03	3.18 \pm 0.57	1.30 \pm 0.16
70	251.70 \pm 23.81	0.21 \pm 0.01	-0.16 \pm 0.01	2.68 \pm 0.16	1.26 \pm 0.05
80	259.15 \pm 24.53	0.18 \pm 0.01	-0.14 \pm 0.02	2.29 \pm 0.19	1.21 \pm 0.07
90	265.72 \pm 24.16	0.15 \pm 0.01	-0.11 \pm 0.02	1.99 \pm 0.24	1.06 \pm 0.04
130	286.25 \pm 27.16	0.07 \pm 0.01	-0.05 \pm 0.02	1.37 \pm 0.08	1.21 \pm 0.07

(b)					
$\sqrt{s}(A\text{GeV})$	$T(\text{MeV})^*$	μ_q/T^*	μ_s/T	Ω^+/Ω^-	Ξ^+/Ξ^-
20			-0.03 \pm 0.09	1.16 \pm 0.60	0.41 \pm 0.14
30			-0.11 \pm 0.08	1.97 \pm 0.95	0.68 \pm 0.22
40			-0.13 \pm 0.05	2.15 \pm 0.64	0.89 \pm 0.18
50			-0.15 \pm 0.04	2.43 \pm 0.58	1.00 \pm 0.16
60			-0.14 \pm 0.03	2.34 \pm 0.42	1.07 \pm 0.13
70			-0.13 \pm 0.03	2.18 \pm 0.33	1.10 \pm 0.11
80			-0.12 \pm 0.02	2.00 \pm 0.24	1.11 \pm 0.09
90			-0.10 \pm 0.02	1.83 \pm 0.22	1.28 \pm 0.10
130			-0.05 \pm 0.01	1.38 \pm 0.05	0.92 \pm 0.03

*The same fitted $T, \mu_q/T$ values as in (a).

ratio $\Omega^+/\Omega^- = e^{-6\mu_s/T}$ becomes larger than unity. We find, within the variance of the extrapolation and the different R_d curves that, at about $\sqrt{s} \sim 50 A\text{GeV}$, both ratios attain their largest values $\sim (2 - 4)$ and $\sim (1 - 1.5)$ for Ω^+/Ω^- and Ξ^+/Ξ^- , respectively, compared to the maximum value of 1 and 0.55, respectively, for the case where $\mu_s = 0$, Table 2. The observation of the above predictions is contingent on the assumption that the T, μ_q, μ_s values of the primordial equilibrated state are conserved until hadronization and thus can be deduced from the particle yield ratios (see discussion below).

7. Summary and Discussion

We have shown that the existence of an intermediate region of deconfined, massive and correlated quarks, in-between the hadronic and chiral quark-gluon phases, is realistic and within the results of recent lattice and effective Lagrangian calculations. We have constructed an empirical EoS for the DQM phase, in terms of the order parameters and the mass-scaled partition functions of the HG and QGP phases, from which a

relation for the strange-quark chemical potential is obtained in terms of μ_q and T . This empirical EoS includes mass-scaled strange hadrons, approximating the effects of the progressive decrease of the interaction-correlation with increasing temperature, as well as a mass-scaled QGP term. In effect, it describes realistically the gross features of the dynamics and characteristics of the DQM phase. The EoS indicates that an unambiguous and concise characteristic observable of this phase is the large negative strange-quark chemical potential. It also shows that μ_s may possibly be considered and used as an experimentally accessible order parameter of the deconfinement phase transition, the only such parameter proposed up to now.

Negative chemical potential appears also in condensed matter systems. For example, in a transition between weakly coupled Cooper pairs, with $\mu > 0$ and the usual BCS superconducting gap $|\Delta k|$, and the strongly coupled diatomic pairs, with $\mu < 0$ and the corresponding gap $(\Delta k^2 + \mu^2)^{1/2}$, representing an insulating system [31]. The analogy with the baryon-dense nuclear matter case is rather the opposite. The positive strange-quark chemical potential ($\mu_s > 0$) corresponds to a colour insulator (hadron gas state), whereas $\mu_s < 0$ to a colour (super)conductor (deconfined partonic state). An even simpler system, such as an ideal, three dimensional Bose gas, has also a well defined chemical potential as we move above the Bose - Einstein condensation critical temperature, where $\mu < 0$, or below this critical point, where $\mu = 0$.

An important argument of this work is that the light and strange quark fugacities λ_q and λ_s , as well as the temperature are attributed to the equilibrated primordial state, to which Eq's (1,12) refer. Only in this case one would expect to observe negative strange-quark chemical potential and temperature in excess of those corresponding to deconfinement, for a state beyond the HG phase. This appears at first as "impossible", since hadronization always takes place on the deconfinement-hadronization line, separating the HG phase from the DQM and, therefore, these quantities should attain values only on this line. That is, always $\mu_s = 0$, and for the sulfur-induced interactions for example, which have $\mu_q \sim 80 \text{ MeV}$, a temperature $T \sim 176 \text{ MeV}$ [15, 21].

To overcome this apparent difficulty, we propose without proof that the conservation of fugacities λ_i ($i = u, d, s$) is a characteristic property of strong interactions and thermodynamic equilibration in general, affecting thermally and chemically equilibrated states throughout the phase diagram. That is, the quark fugacities λ_i , once fixed in a chemically equilibrated primordial state, are constants of the entire sequent evolution process. This is contingent on an isentropic expansion and hadronization via a sudden, fast process without mixed phase. The relation between λ_i and T , and hence between μ_i and T in the primordial state§ is defined by the strangeness neutrality equation, obtained from the partition function by imposing strangeness conservation. The proof of the fugacity conservation ansatz will require a precise knowledge of the EoS of the DQM state, so that the variation of the volume, quark density, temperature, chemical

§ The quantities μ_s, μ_q and T are the Lagrange multipliers of strangeness, baryon number and energy, attaining their values in the equilibrated state.

potentials and entropy can be studied from equilibration to hadronization. This is beyond the scope of the present paper. It is only stated here in order to give a possible explanation of an observation of negative strange-quark chemical potential, which is not a characteristic of the hadronic phase, as well as of temperatures higher than the maximum temperature for deconfinement ($T_d \sim 175 \text{ MeV}$ at $\mu_q \sim 80 \text{ MeV}$, as given by SSBM). For the latter, there might be already such an observation in the $S + S$ interactions at 200 AGeV , as discussed earlier. If proven true, the above statements would have far-reaching consequences for defining and understanding the thermodynamic characteristics of the primordial state. They would suggest that, if nuclear interactions create equilibrated states beyond the HG phase in the deconfined region with finite net baryon number density, if the path to hadronization is isentropic and if the confinement transition is explosive without a mixed phase, one may determine the thermodynamic quantities of the state from the strange hadron yields, by employing an appropriate EoS. If negative μ_s -values, together with temperatures in excess of T_d are confirmed at the proposed RHIC energies of $20 < \sqrt{s} < 100 \text{ AGeV}$, it will be a profound observation. It will indicate that negative strange-quark chemical potential is indeed a unique and well-defined signature of deconfinement, identifying the partonic phase, and that μ_s is the first experimentally accessible order parameter of deconfinement. Of equal importance will be the ability to determine the quantities μ_q , μ_s and T , hence, to calculate accurately the energy density and entropy of equilibrated primordial states situated beyond the hadronic phase, in the deconfined-quark region.

On the basis of the present analysis we also conclude that the $S + S$ collision at 200 AGeV at the SPS may be the first interaction to have produced an equilibrated partonic state beyond the hadronic phase. On the other hand, the thermodynamic parameters of the primordial state of the $Pb + Pb$ interaction at the highest energy of 158 AGeV strongly indicate that its location is well within the hadronic phase.

Appendix A. Order parameters and the phase diagram

Since an empirical partition function for the DQM phase is used, Eq. (12), containing the parameters $R_d(T)$ and $R_\chi(T) \equiv 1 - R_d(T)$, it is important to study the behaviour of the strange-quark chemical potential in the DQM region for the different approximations of $R_d(T)$. Figure A.1 is a plot of μ_s vs. T , obtained for $\mu_q = 0.45T$ and the two different functions for $R_d(T)$. It is clear that the DQM region is characterized by negative strange-quark chemical potential, independently of which $R_d(T)$ function is used in the EoS. Therefore, the change in the sign of the strange-quark chemical potential, from positive to negative, is a unique and well-defined indication of the quark-deconfinement phase transition and does not depend on the phenomenological parameters of the model.

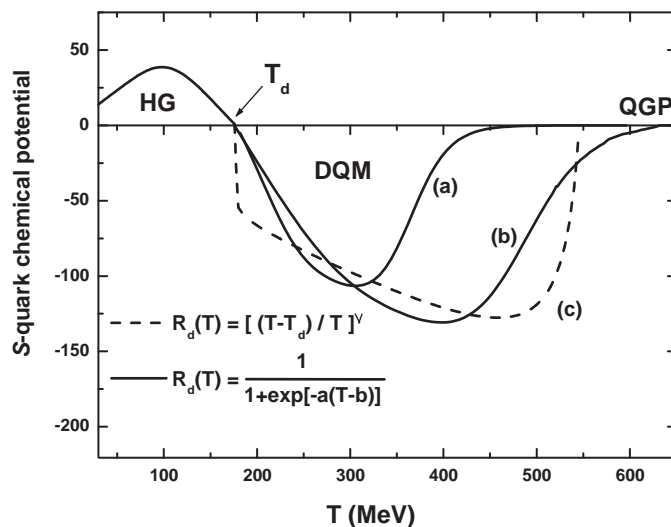


Figure A1. Plot of the strange-quark chemical potential as a function of the temperature and the two different functions for $R_d(T)$, obtained for (a) $\alpha = 0.05$, $\beta = 229$, (b) $\alpha = 0.03$, $\beta = 268$ with Eq. (7) and (c) for $\nu = 0.1$ with Eq. (8), respectively.

Appendix B. Order parameters and the effective quark masses

The parameter $R_\chi(T)$ determines the effective quark and hadron masses. The use of temperature dependent quark masses is one of the essential aspects of the model, since it is a dynamical term in the equation of state. On the other hand, more precise theoretical models such as the NJL or the (non)linear sigma model, have also studied the temperature dependence of the light and strange quark masses. Figures B.1, B.2 plot the strange and light quark masses as a function of temperature, using the two different approximations of the order parameter, whereas Figure B.3 exhibits the same quantities but within the NJL model. The quark mass scaling used in our model is

consistent with the results of an effective field theory model, despite the difference for m_s^* , which can be corrected by choosing an appropriate $R_\chi(T)$ for strange quarks. This gives strong support to our approximations and results.

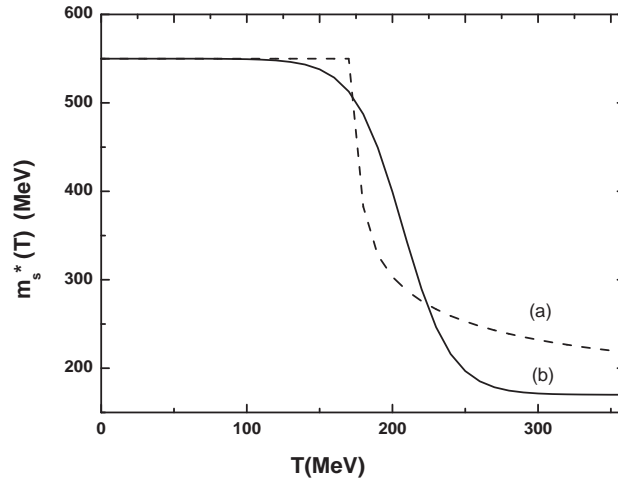


Figure B1. The effective quark mass $m_s^*(T)$ calculated using the expressions of Eq.(8) with $\nu = 0.2$, $c = 1$ in (a) and Eq.(7) with $\{\alpha = 0.03, \beta = 268\}$ in (b).

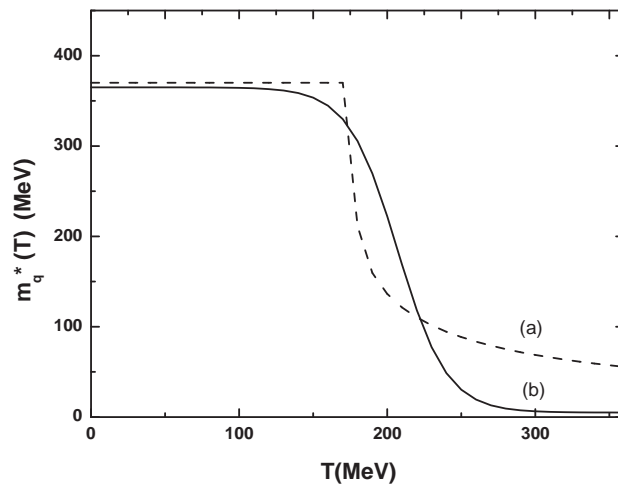


Figure B2. The effective quark mass $m_q^*(T)$ calculated using the expressions of Eq.(8) with $\nu = 0.2$, $c = 1$ in (a) and Eq.(7) with $\{\alpha = 0.03, \beta = 268\}$ in (b).

References

- [1] Marciano W, Pegels H, *Phys. Rep.* **36**, 137 (1978)
- [2] Shuryak E V, *Phys. Lett.* **B107**, 103 (1981)
Pisarski R D, *Phys. Lett.* **B110**, 155 (1982)
- [3] H. Satz, *Nuovo Cim.* **A37**, 141 (1977)
- [4] Panagiotou A D, Mavromanolakis G, Tzoulis J, *Proc. Int. Conf. "Strangeness in Hadronic Matter"*, 449 (1995)
- [5] Panagiotou A D, Mavromanolakis G, Tzoulis J, *Strangeness '96 Conf.*, Budapest, *Heavy Ion Physics* **4**, 347 (1996)
- [6] Panagiotou A D, Mavromanolakis G, Tzoulis J, *Phys. Rev.* **C53**, 1353 (1996)
- [7] Karsch F, *Nucl. Phys.* **A698**, 199 (2002)
- [8] Asprouli M N and Panagiotou A D, *Phys. Rev.* **D51**, 1086 (1995)
- [9] Kapoyannis A S, Ktorides C N and Panagiotou A D, *J. Phys.* **G23**, 921 (1997)
- [10] Engels J, Kaczmarek O, Karsch F and Laermann E, *Nucl. Phys.* **B558**, 307 (1999)
- [11] Satz H, *Proc. XXIII International Conference on High Energy Physics*, Berkeley 16-23 July 1986, ed. S.C. Loken World Scientific Singapore
- [12] Kajantie K and Kapusta J, *Ann. Phys. NY* **160**, 477 (1985)
- [13] Klevansky S P, *Rev. Mod. Phys.* **64**, 649 (1992)
- [14] Cabbibo N, Parisi G, *Phys. Lett.* **B59**, 67 (1975)
- [15] Kapoyannis A S, Ktorides C N, Panagiotou A D, *Phys. Rev.* **C58**, 2879 (1998)
- [16] Katsas P *et al*, *work in progress*
- [17] Ahle L *et al* (E-802 Collaboration), *Phys. Rev.* **C57**, 466 (1998); *Phys. Rev.* **C60**, 044904 (1999)
- [18] Bachler J *et al* (NA35 Collaboration), *Z. Phys.* **C58**, 367 (1993)
Alber T *et al* (NA35 Collaboration), *Z. Phys.* **C64**, 195 (1994)
- [19] Afanasiev S V *et al* (NA49 Collaboration), *Phys. Lett.* **B491**, 59 (2000)
Afanasiev S V *et al* (NA49 Collaboration), *J. Phys.* **G27**, 367 (2001)
- [20] Kapoyannis A S, Ktorides C N and Panagiotou A D, *Phys. Rev.* **D58**, 034009 (1998)
- [21] Kapoyannis A S, Ktorides C N and Panagiotou A D, *Eur. Phys. J.* **C14**, 299 (2000)
- [22] Kapoyannis A S, Ktorides C N and Panagiotou A D, *J. Phys.* **G28**, L47 (2002)
- [23] Becattini F, *J. Phys.* **G23**, 1933 (1997)
- [24] Sollfrank J, *J. Phys.* **G23**, 1903 (1997)
- [25] Becattini F, Gazdzicki M, Sollfrank J, *Eur. Phys. J.* **C5**, 143 (1998)
- [26] Becattini F, Cleymans J, Redlich K, *Phys. Rev.* **C64**, 024901 (2001)
- [27] Cleymans J, Redlich K, *Phys. Rev.* **C60**, 054908 (1999)
- [28] A. D. Panagiotou, P. G. Katsas, E. Gerodimou *J. Phys.* **G28**, 2079 (2002)
- [29] Hagedorn R, *Riv. Nuov. Cim.* **6**, 1 (1983) ; *Proc. Advanced NATO workshop: Hot Hadronic Matter. Theory & Experiment*, Divonne-les-Bains July 1994, ref's therein.
- [30] Braun-Munzinger P, Magestro D, Redlich K and Stachel J, *Phys. Lett.* **B518**, 41 (2001)
- [31] Mouloupoulos K and Ashcroft N W, *Phys. Rev.* **B42**, 7855 (1990)
- [32] Stock R, *Proc. 18th Winter Workshop on Nuclear Dynamics*, 001-002 (2002) [arXiv:hep-ph/0204032]

This figure "figureB3.jpg" is available in "jpg" format from:

<http://arxiv.org/ps/hep-ph/0212082v1>

This figure "figure6.jpg" is available in "jpg" format from:

<http://arxiv.org/ps/hep-ph/0212082v1>